Waste Rambutan-Derived Porous Carbon Materials Applied to Supercapacitors

Wenbo Liu [1,*], Xiaowen Yu [1,2], Hanhan Wang [1], Wanyi Liao [1], Cong Yong [1] and Wei Liao [1,3]

[1] Chongqing Ceprei Industrial Technology Research Institute Co., Ltd., Chongqing 400000, China
[2] Automotive Electronic Components Safety and Reliability Technology and Evaluation Chongqing Key Laboratory of Industry and Information Technology, Chongqing 400000, China
[3] Chongqing Key Laboratory of Reliability Technologies for Smart Electronics, Chongqing 400000, China

Abstract. The supercapacitor, as a novel energy storage device, possesses the advantages of rapid charging and discharging, extended cycle life, high power density, low energy density, excellent voltage resistance, large capacity, and more. Biomass serves as an ideal electrode material for supercapacitors due to its high carbon content, cost-effectiveness, and environmental friendliness. In this study, waste rambutan peel is utilized as the raw material and subjected to KOH activation following high-temperature pyrolysis to fabricate porous carbon materials with well-ordered pore size distribution. The rambutan peel electrode material exhibits a mass-specific capacitance of 285 F g^{-1} (at 1 A g^{-1} current density) and retains 105% after 5000 cycles of charge and discharge. This provides a direction for the reuse of biomass materials.

1 Introduction

Amidst the rapid expansion of the global economy and the continuous growth of the world population, nonrenewable energy such as coal and oil are overconsumed, which has brought serious environmental problems. Supercapacitors are a type of emerging energy storage devices that have been garnering increasing attention from the global renewable energy industry. It has a higher specific capacity and higher power density than ordinary capacitors and has faster charge and discharge speed and longer cycle life than ordinary capacitors [1]. Compared with lithium-ion batteries, supercapacitors are safer and will not cause explosion, fire, electrolyte leakage and other problems. Supercapacitors have excellent performance and broad development prospects in power generation, smart grid, and portable electronic products [2].

Carbon materials are commonly utilized as electrode materials in supercapacitors. Currently, a diverse range of carbon materials have been employed, including activated carbon, carbon nanotubes, and graphene. These carbon materials have a high specific surface area, so they can provide high specific energy and high power. Biomass production in the world is extremely rich, reaching 450 million tons per year. Biomass, with its high carbon content and low cost, makes an ideal carbon source. In addition, biomass contains rich oxygen-containing functional groups, and some biomass itself contains natural pore structure, which will have natural advantages in the preparation of porous carbon materials, and the properties of the prepared carbon materials will also be better than the traditional carbon materials [3].

In this study, waste rambutan peel was utilized to prepare porous carbon with an ordered porous structure through high-temperature pyrolysis following KOH activation. The specific capacitance of the rambutan peel electrode material was 285 F g^{-1}. Following 5000 cycles of charge and discharge, the retention rate reached 105%. The activation treatment of waste rambutan peel resulted in the production of rich specific surface area and n-doped biomass carbon materials, leading to a significant improvement in the electrochemical performance of the use of supercapacitors.Fig. 1 shows the material preparation process in this study.

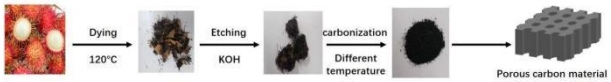

Fig. 1. The preparation process of rambutan-derived porous carbon materials.

2 Experiment

2.1 Preparation of KC-N carbon materials

The peel of rambutan was washed and dried at 120℃ for 24 hours. The dried pericarp was chopped and ground in a mortar, then heated with 3M KOH at 120 ℃ for 12 hours to obtain a preliminary activated rambutan pericarp. The impurities in the product were washed with 100 ml of 1 M HCl solution and then dried. The obtained product is annealed at different temperatures in a tubular furnace under nitrogen protection. The obtained product

* Corresponding author: liuwb96@163.com

is named KC-N (N=500℃,600℃,700℃,800℃).

2.2 Preparation of KC-N electrodes

The working electrode was prepared by mixing KC-N, carbon black (CB), and polyvinylidene fluoride (PVDF) at a mass ratio of 8:1:1. Several drops of N-methyl pyrrolidone (NMP) were added to the mixture, which was then ground for several minutes until evenly mixed. The mixture was then evenly coated on the surface of graphite paper, and the KC-N electrode was obtained by vacuum drying overnight at 100℃.

3 Results and discussion

Characterization of the materials was obtained by scanning electron microscopy (SEM, JEOL JEM6380LV), Raman spectrometer (Dilor's SuperLabram II), Physical Adsorber (ASAP 2020M), and X-ray photoelectron spectroscopy (XPS, PHI-5000 Versa Probe II).

Electrochemical performance was tested by CHI660C electrochemical analysis system (Chenhua, Shanghai China).

The test solution is 1 mol L^{-1} KOH, and the voltage window is -0.7V ~+ 0.2V. Electrochemical performance calculation formula (Table 1 shows the meaning and units of symbols in the formula):

$$C = \frac{I \times \Delta t}{m \times \Delta V} \quad (1)$$

Table 1. Symbolic meaning in the formula.

Symbol (unit)	name
I(A)	discharge current
△t(s)	discharge time
m(g)	total mass of working electrode
△V(V)	scanning voltage window
C(F g^{-1})	specific capacitance

3.1 Material characterization

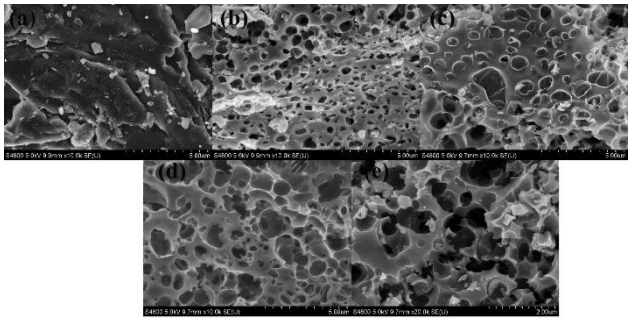

Fig. 2. (a) SEM image of C-700, (b-e) SEM images of KC-500,KC-600,KC-700,KC-800.

Fig. 2a shows the SEM image of carbon material prepared from rambutan peel without activation treatment. The figure shows that the non-activated pyrolytic carbon material is a lamellar material with a smooth surface and no obvious voids. Figs. 2b-2e exhibit the SEM spectrums of porous carbon material produced from rambutan peel after KOH activation and subsequent annealing at varying temperatures. The figures indicate that a loose, porous three-dimensional network with a rich pore structure is formed following KOH activation. The pore structure on the material surface becomes increasingly abundant as the carbonization temperature changes. As the temperature increases from 500 ℃ to 800 ℃, the three-dimensional network structure becomes looser, and the surface becomes smoother. Thus, it can be inferred that the carbon material derived from rambutan peel undergoes graphitization as the pyrolysis temperature increases. However, at 800 ℃, the porous carbon structure collapses, indicating that the ideal activation temperature is 700 ℃.

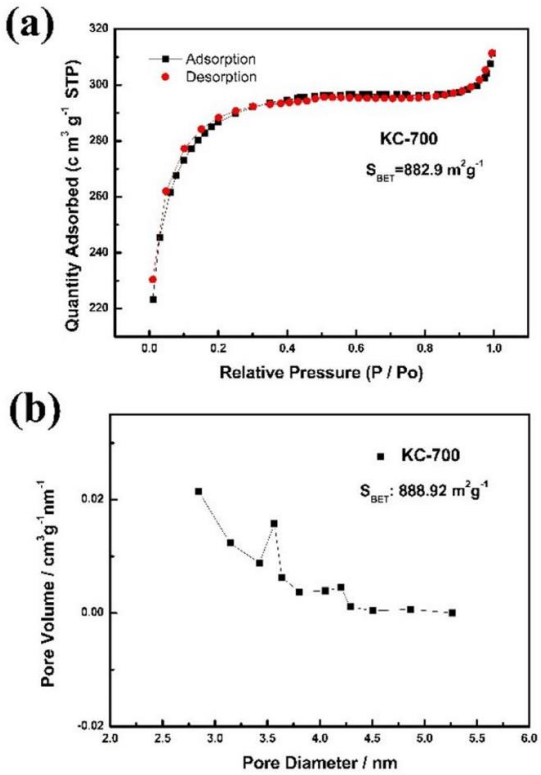

Fig. 3. (a) Nitrogen adsorption-desorption isotherm of KC-700, (b) pore size distribution diagram of KC-700.

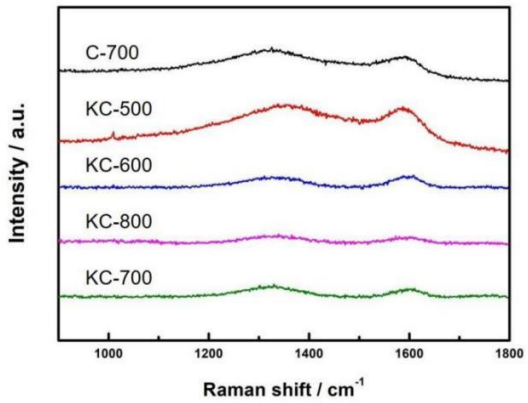

Fig. 4. Raman spectra of rambutan-derived carbon materials.

The N_2 adsorption-desorption isotherm curve of

KC-700 and the pore size distribution of KC-700 are shown in Fig. 3. From Fig. 3a, it can be observed that the nitrogen adsorption-desorption type of KC-700 is the first type of adsorption/desorption curve. The relative pressure (p/p0) curve rises abruptly in the 0~0.1 region, indicating the presence of a few micropores and an uneven pore structure. The specific surface area of KC-700 was 882.90 m2 g^{-1}, which was much higher than that of C-700 (29.70 m2 g^{-1}). From Fig. 3b, we find that the material has mesopores, and the pore size of KC-700 ranges from 3 to 5 nm. The appropriate pore size distribution, mesoporous structure, and large specific surface area facilitate ion diffusion and migration [4].

Fig. 4 shows the Raman spectra of C-700 and KC-N. the Raman spectra further explore the microstructure of rambutan peel-derived carbon materials. The broad peak at 1330 cm^{-1} corresponds to the D-band, indicating the degree of defects or amorphousness. The wide peak at 1585 cm^{-1} corresponds to the G-band, indicating the degree of graphitization. The ratio of the D-band strength to the G-band strength (ID/IG) represents the graphitization degree of the carbon material derived from rambutan peel [5]. The numerical ratio of the intensity of the D-band diffraction peak and the intensity of the G-band diffraction peak of rambutan peel-derived carbon material is calculated. The ID/IG values of C-700, KC-500, KC-600, KC-700, and KC-800 are 1.25, 1.05, 1.08, 1.45, and 1.27 respectively. With the change in activation temperature, the ID/IG value of rambutan peel-derived carbon materials increased first and then decreased. At high temperatures, the structure of rambutan peel-derived carbon materials was unstable and collapsed, resulting in excessive defects in disordered structures. 700 ℃ is the best activation temperature, which is consistent with the SEM results.

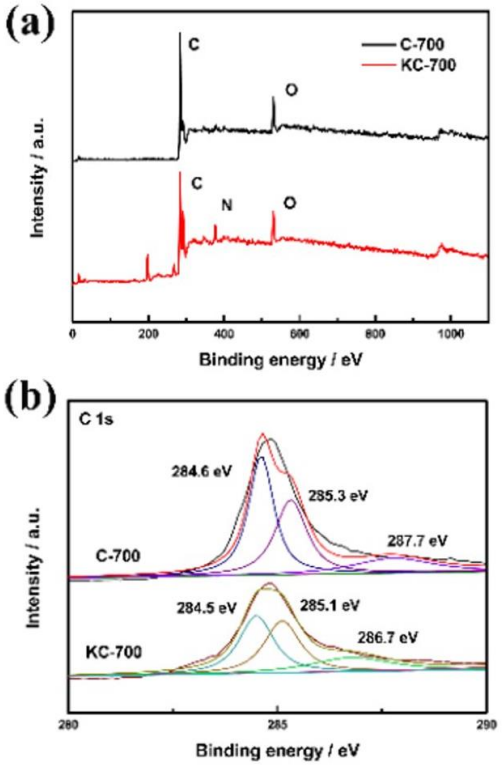

Fig. 5. (a) Full XPS spectra of C-700 and KC-700, (b) C-1S diagram of C-700 and KC-700.

Fig. 5a shows the XPS spectra of C-700 and KC-700. From the spectra, we can find that the material activated by KOH has one more characteristic peak, and the analysis shows the characteristic spectra of N element. Compared with traditional activated carbon materials, the wettability of N-doped materials has changed, and the adsorption ability of the material to charge has increased. We classified several characteristic carbon peaks of C-700 (Fig.5b) as follows: C=C (284.6eV), C-O (285.3eV), OH-C = O (287.7eV). It can be found from the atlas that the characteristic peaks of KC-700 material after KOH activation are: The characteristic peaks at C=C (284.5eV), C-O (285.1eV), O-C (286.7eV), OH-C = O (287.7eV) disappear and O-C (286.7eV) appears, indicating that the C element in the material changes from sp^3 hybrid to sp^2 hybrid. KOH activation increased the graphite phase C content of the material, which provided a strong support for improving the electrochemical properties of the material.

3.2 Electrochemical Characterization

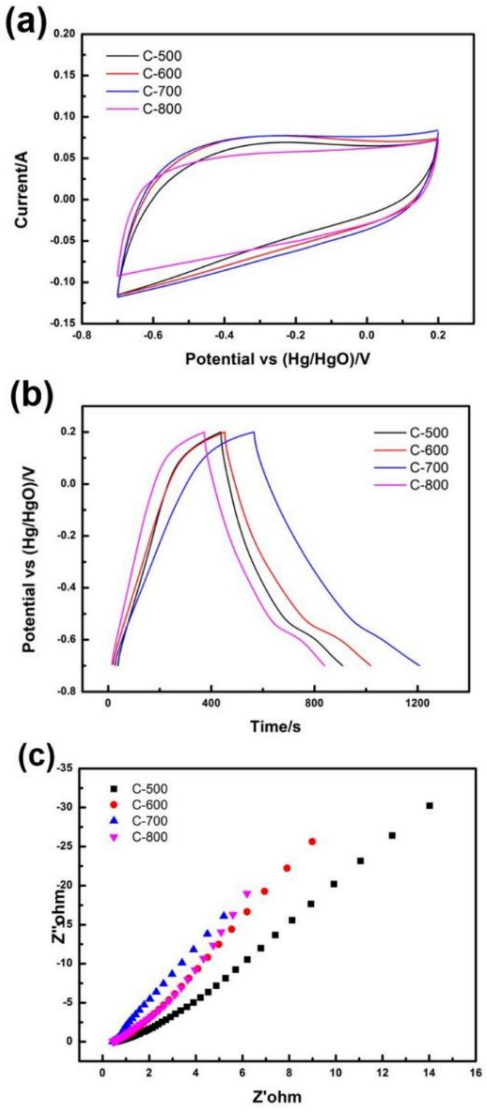

Fig. 6. (a) Comparison of CV curves, (b) Comparison of GCD curves, (c) Nyquist curves.

Fig. 6a is the CV Curve of KC-N at the scanning rate of 100 mV s^{-1}. The CV shapes of KC-N all present oval-like rectangular shapes, and KC-700 has the largest area. The GCD curves of KC-N in Fig. 6b show linear and approximately symmetrical characteristics. Compared with the discharge time, it is consistent with the CV Curve. The specific capacitance values of C-700, KC-500, KC-600, KC-700 and KC-800 are 80, 117, 172, and 164 F g^{-1} respectively, according to the formula.The results showed that KOH activation increased the capacitance of rambutan-derived carbon materials, and 700 ℃ was the best pyrolysis condition for rambutan-derived carbon materials. Fig. 6c is the Nyquist curve of KC-N. KC-700 has the minimum Rs value, and the curve of KC-700 in the low-frequency region is 90 ° from the coordinate axis. This makes KC-700 an ideal material for capacitors due to the three-dimensional porous network structure of rambutan-derived carbon materials and the increase in graphitized carbon [6].

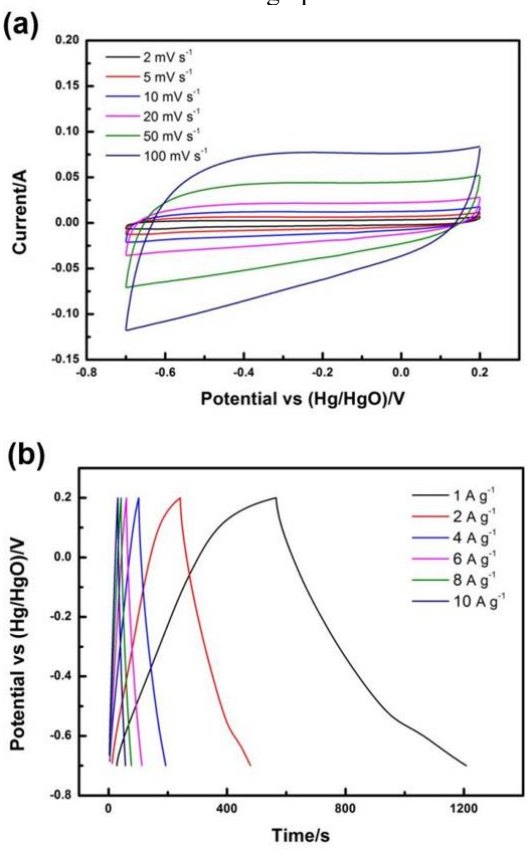

Fig. 7. (a) CV curves of KC-700, (b) GCD curves of KC-700.

Figs. 7a and 7b show the CV and GCD curves of KC-700 at different scanning speeds and current densities in the three-electrode system. The shape of the CV Curve and GCD curve can remain unchanged even at high scanning speed and high current density, indicating that the material has good capacitive performance. The increase in specific capacitance is attributed to the etching effect of KOH. The carbon material derived from rambutan has a complex pore structure and an expanded specific surface area. Doping N element increases the wettability of the material and the graphite phase of the material [7]. A high specific surface area is beneficial for improving the charge and ion transfer rate, while the material's porous structure can create more space for charge storage.

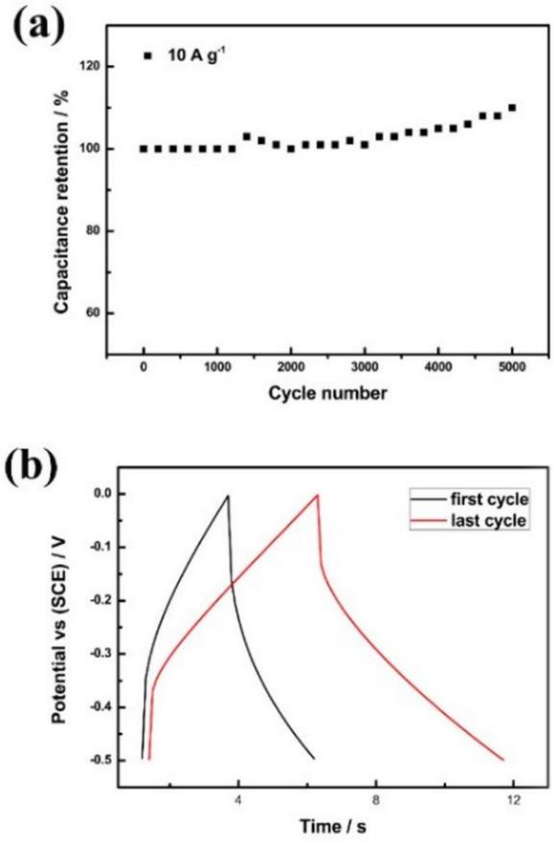

Fig. 8. (a) Capacity retention rate of KC-700 after 5000 cycles, (b) The GCD curves of the first loop and the last loop.

We investigated the cycle stability of carbon materials derived from rambutan. Fig. 8a shows the capacity retention rate of KC-700 after 5000 charge and discharge (10 A g^{-1}) in KOH electrolyte, and Fig. 8b shows the GCD curve comparison of first cycle and last cycle. After 5000 cycles, the capacitance retention rate of the material can reach 105%, and the GCD image shape of the first test and the last test remains unchanged, which reflects that the material has good cycle performance. The improved electrochemical performance is attributed to the activation of electrolytes [8].

4 Conclusion

The porous carbon material was prepared through KOH activation and high-temperature carbonization pyrolysis of rambutan peel biomass. The optimal reaction and pyrolysis condition is at 700 ℃, resulting in a specific capacitance of KC-700 up to 285 F g^{-1}. The outstanding electrochemical properties of the material are attributed to 1) the transformation of the sample surface from smooth to rough after KOH activation, leading to the formation of a porous three-dimensional network structure with abundant pore structure; 2) the presence of mesoporous pores, appropriate pore size distribution, and

large specific surface area facilitating ion diffusion and migration; 3) N doping provided by biomass materials altering wettability compared to traditional activated carbon materials, thereby enhancing charge adsorption capacity.

References

1. Guo, Z.; Han, X.; Zhang, C.; He, S.; Liu, K.; Hu, J.; Yang, W.; Jian, S.; Jiang, S.; Duan, G. J. C. C. L., Activation of biomass-derived porous carbon for supercapacitors: A review. **2023**, 109007.
2. Ashok Kumar, S. S.; Bashir, S.; Pershaanaa, M.; Kamarulazam, F.; Saidi, N. M.; Goh, Z. L.; Ma, I. W.; Kunjunee, V.; Jamaluddin, A.; Ramesh, K. J. J. o. M. S., A review on the recent progress of the plant-based porous carbon materials as electrodes for high-performance supercapacitors. **2023,** *58* (15), 6516-6555.
3. Sun, Y.; Shi, X. L.; Yang, Y. L.; Suo, G.; Zhang, L.; Lu, S.; Chen, Z. G., Biomass-Derived Carbon for High-Performance Batteries: From Structure to Properties. *Advanced Functional Materials* **2022,** *32* (24).
4. Qiu, G.; Miao, Z.; Guo, Y.; Xu, J.; Jia, W.; Zhang, Y.; Guo, F.; Wu, J. J. C.; Physicochemical, S. A.; Aspects, E., Bamboo-based hierarchical porous carbon for high-performance supercapacitors: the role of different components. **2022,** *650*, 129575.
5. Hao, J.; Wang, X.; Wang, Y.; Lai, X.; Guo, Q.; Zhao, J.; Yang, Y.; Li, Y. J. N. A., Hierarchical structure N, O-co-doped porous carbon/carbon nanotube composite derived from coal for supercapacitors and CO 2 capture. **2020,** *2* (2), 878-887.
6. Luo, L.; Zhou, Y.; Yan, W.; Wu, X.; Wang, S.; Zhao, W. J. E. A., Two-step synthesis of B and N co-doped porous carbon composites by microwave-assisted hydrothermal and pyrolysis process for supercapacitor application. **2020,** *360*, 137010.
7. Liu, W.; Li, H.; Du, T.; Guo, J.; Zhang, S.; Lu, Y. J. D.; Materials, R., A porous carbon-based composite PPC@ co-NCNT derived from pomelo Peel as a flexible self-supporting electrode for supercapacitors. **2023,** *135*, 109892.
8. Sarkar, S.; Arya, A.; Gaur, U. K.; Gaur, A. J. B.; Bioenergy, Investigations on porous carbon derived from sugarcane bagasse as an electrode material for supercapacitors. **2020,** *142*, 105730.